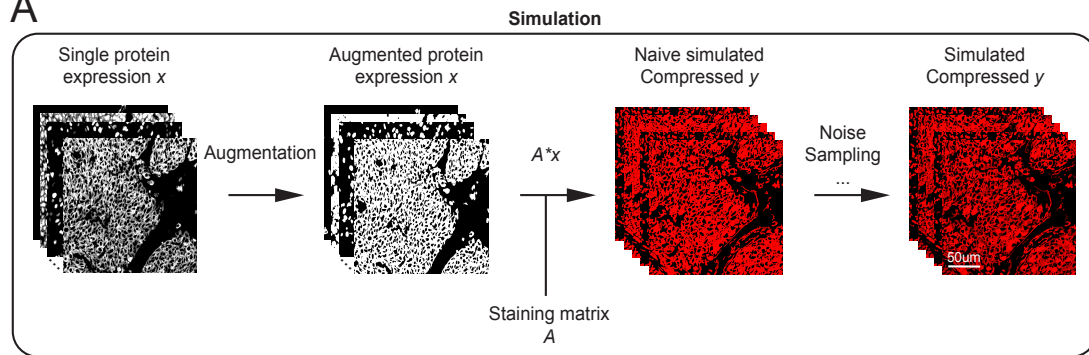
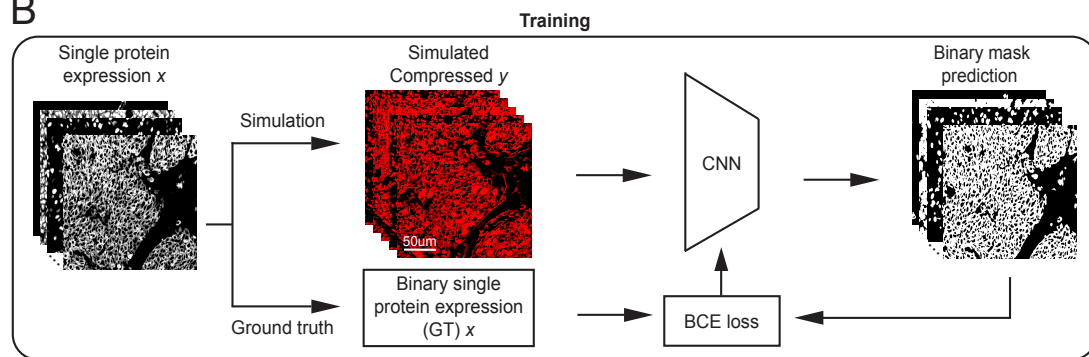
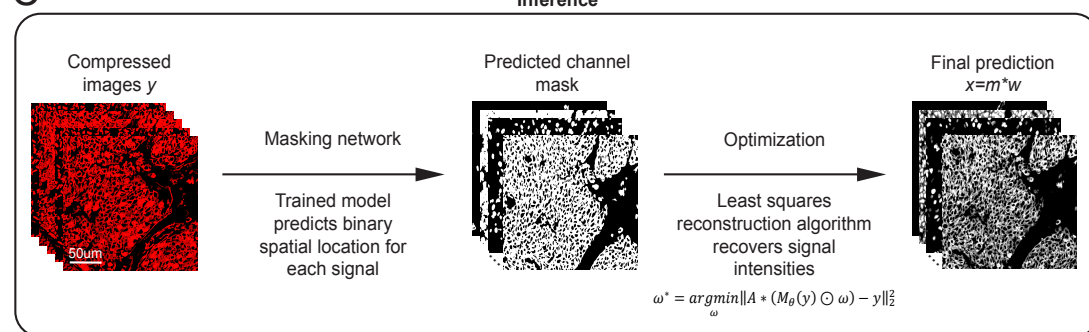
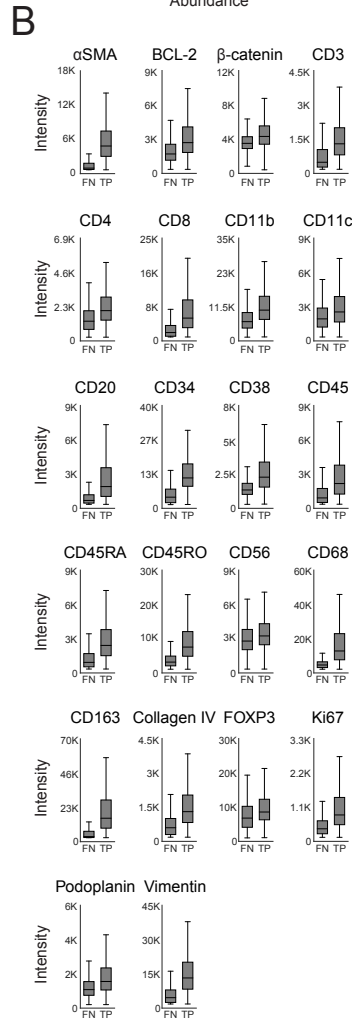
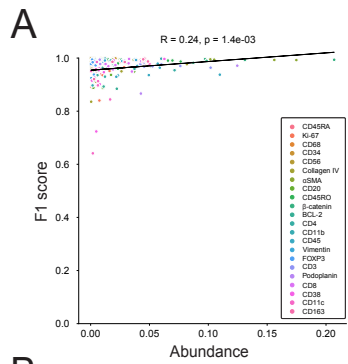


A**B****C**

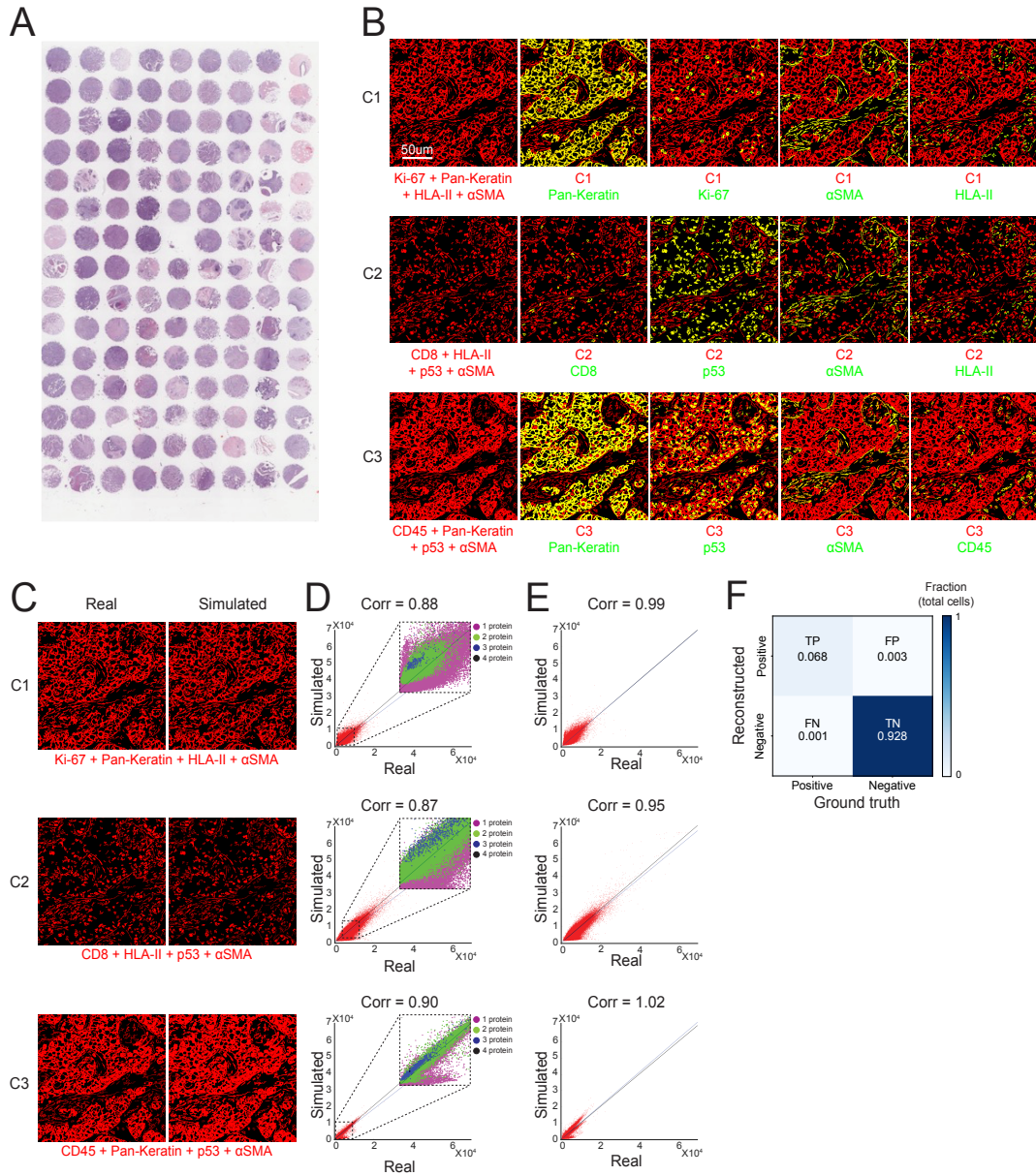
Supplementary figure 1: Algorithmic overview of CombPlex

(A) Illustration of the simulation process of compressed images. **(B)** Illustration of the training process involving simulated compressed images. The loss is calculated by comparing binarized masks of the single-protein images and the binary mask predictions generated by the neural network, using the compressed images as input. **(C)** Illustration of the inference procedure. compressed images are provided as input and undergo a two-step algorithm: the masking network and optimization phase.

Supplementary figure 2: Analysis of simulations

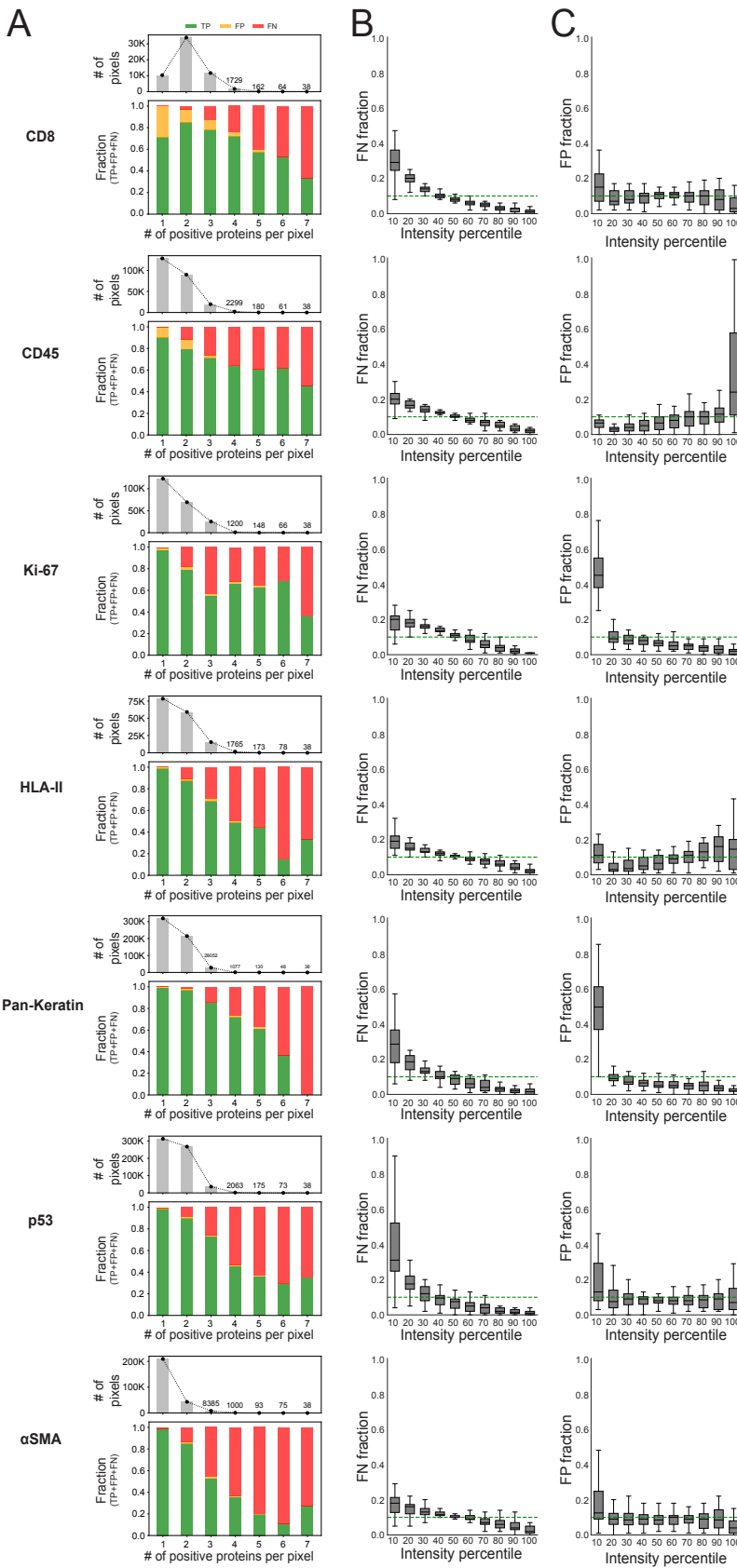


(A) The data from Schurch et al¹ was used to simulate combinatorically-compressed images and to decompress them using CombPlex. Shown is the correlation between the F1 score (y-axis) of different proteins and their abundance (x-axis) on a test set of 8 FOVs. **(B)** Shown are the intensity values in ground truth images (y-axis) of FN and TP pixels (x-axis) for 22 proteins on a test set of 8 FOVs. FN errors tend to have lower intensities than TP pixels.



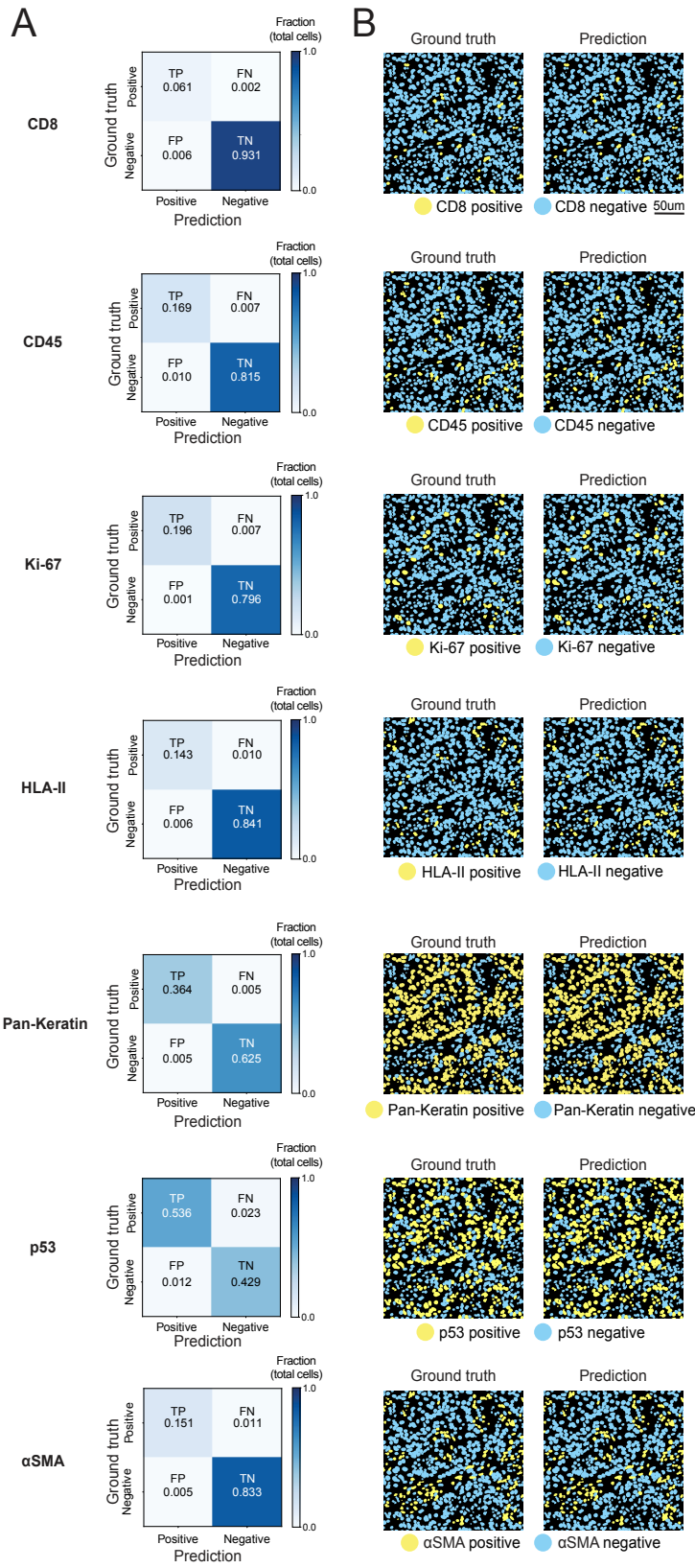
Supplementary figure 3: Evaluation of CombPlex on CODEX experiments

(A) A TMA of 132 breast carcinoma cores. Samples were used to generate compressed and ground truth images. **(B)** Overlay of seven experimentally-measured single-protein images (ground truth, green) with the respective compressed images that contain all of their signals (red). Yellow pixels indicate overlap. **(C)** Side-by-side comparison of experimentally compressed images (left) and simulated compressed images (right). **(D)** Shown is the correlation between the experimentally-compressed and simulated compressed images shown in (C). Inset is colored by the number of overlapping proteins per pixel. **(E)** Shown is the correlation of the images shown in (C), after augmentation of pixel intensities according to the number of overlapping proteins per pixel (Methods). **(F)** For each protein in the 32 test FOVs, each pixel was compared between the ground truth images and the images reconstructed by CombPlex. Pixels were classified as TP, FN, FP and TN.



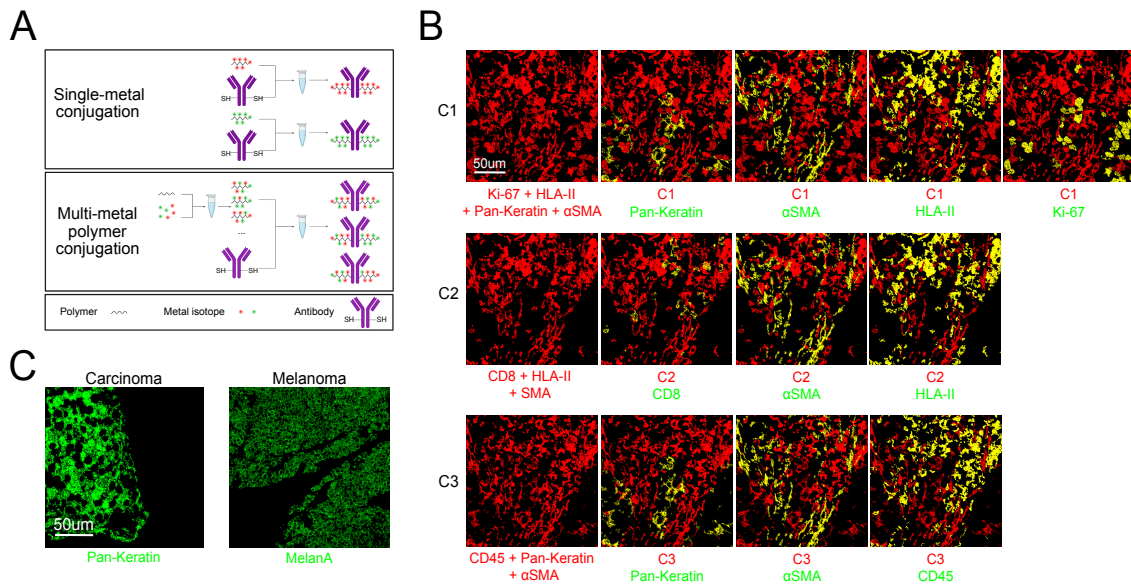
Supplementary figure 4: False Negative and False Positive analysis in CODEX CombPlex experiments

CODEX cyclic imaging was used to image seven proteins on a single tissue section, both compressed, and individually. For each protein are shown: **(A)** Bottom: Shown is the composition of TP (True Positives), FP (False Positives), and FN (False Negatives) pixels (y-axis) across all distinct single-protein images of all FOVs as a function of the number of proteins that are positive in each pixel (x-axis). Top: The number of pixels corresponding to each protein count. **(B)** Shown are the fractions of FN pixels (y-axis) for each decile of GT intensities (x-axis) for all distinct single-protein images across all FOVs. The green line indicates the 0.1 expectation from a uniform distribution. **(C)** Shown are the fractions of FP pixels (y-axis) for each decile of GT intensities (x-axis) for all distinct single-protein images across all FOVs. The green line indicates the 0.1 expectation from a uniform distribution.



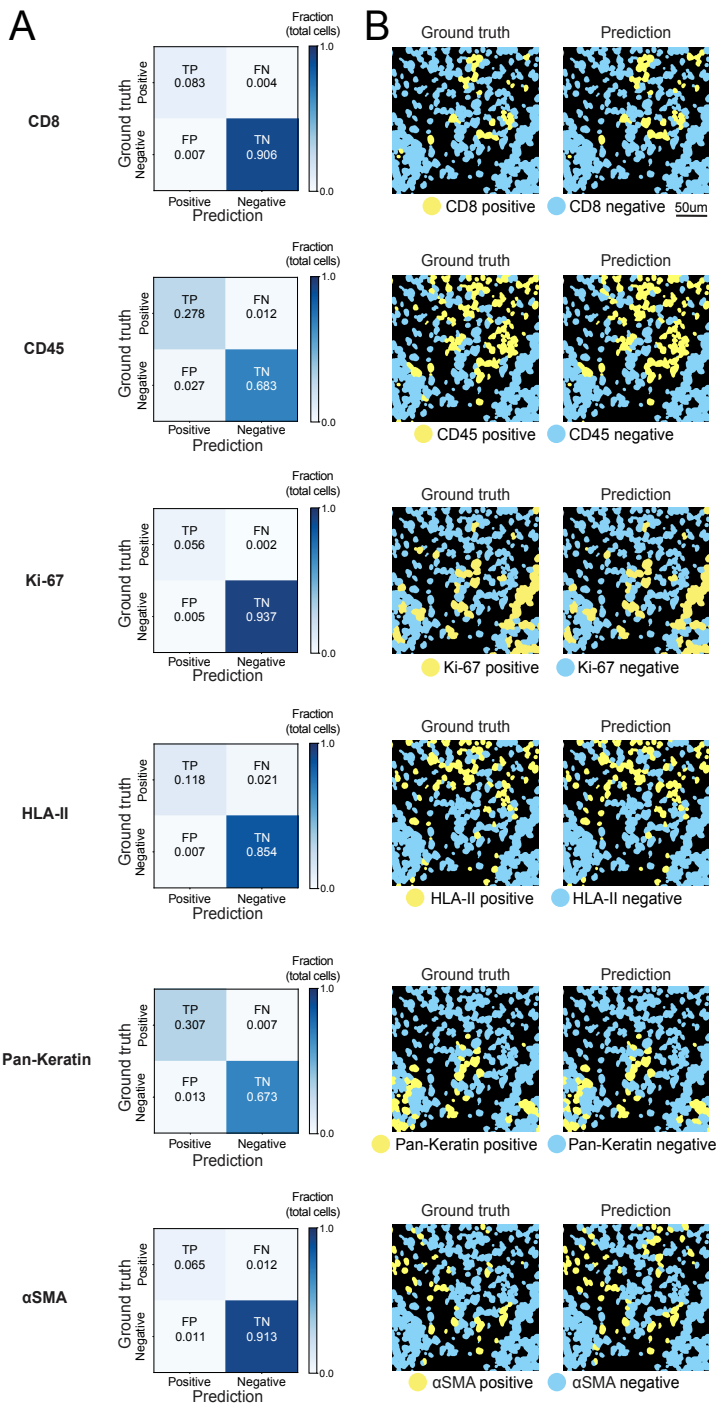
Supplementary figure 5: Classification analysis in CODEX CombPlex experiments

CODEX cyclic imaging was used to image seven proteins on a single tissue section, both combinatorically-compressed, and individually. For each protein (rows), cells were classified as positive or negative based on either the ground truth or reconstructed single-protein image. **(A)** Shown is the confusion between both classification schemes across 32 test FOVs. TP: True Positive, FN: False Negative, FP: False Positive and TN: True Negative. **(B)** Cells classified as positive (yellow) and negative (cyan) for each protein (rows) using ground truth (left) or reconstructed (right) images.



Supplementary figure 6: Evaluation of MIBI-TOF CombPlex experiments

(A) Illustration of metal-conjugation methods. Single-metal conjugation (top): separate lots of the same antibody are reduced and conjugated separately, each to a single-metal labeled polymer. Multi-metal polymer conjugation (bottom): Unlabeled polymers are loaded with multiple isotopes and conjugated to a reduced antibody. **(B)** Overlay of six experimentally-measured single-protein images (ground truth, green) with the respective compressed images that contain all of their signals (red). Yellow pixels indicate overlap. **(C)** Shown are example images of Pan-Keratin and MelanA signals in breast carcinoma and melanoma metastases respectively.



Supplementary figure 7: Classification analysis in MIBI-TOF CombPlex experiments
 MIBI-TOF was used to image six proteins on a single tissue section, both combinatorically-compressed, and individually. For each protein (rows), cells were classified as positive or negative based on either the ground truth or reconstructed single-protein image. **(A)** Shown is the confusion between both classification schemes across 19 FOVs. TP: True Positive, FN: False Negative, FP: False Positive and TN: True Negative. **(B)** Cells classified as positive (yellow) and negative (cyan) for each protein (rows) using ground truth (left) or reconstructed (right) images.